

# Multi-Channel Active Noise Control for Periodic Sources — Indirect Approach <sup>★</sup>

Biqing Wu <sup>a</sup>, Marc Bodson <sup>b</sup>

<sup>a</sup>*Intelligent Control Systems Lab, ECE, Georgia Institute of Technology, 777 Atlantic Dr., Atlanta, GA 30332, U.S.A.*

<sup>b</sup>*Department of Electrical and Computer Engineering, University of Utah, Salt Lake City, UT 84112, U.S.A.*

---

## Abstract

The paper presents a multi-channel active noise control algorithm that is designed to reject periodic signals of unknown frequency. It is based on a so-called indirect approach, where the frequency of the disturbance is estimated in real-time, and the estimate is used in a disturbance rejection scheme designed for a known frequency. Improvements over an earlier algorithm include an extension to multi-channel systems, a better frequency estimation algorithm, and a thorough experimental evaluation. For disturbance rejection, a so-called inverse G algorithm is proposed and its properties are compared through analysis and experiments to those of a gradient algorithm. A new frequency estimator is also considered that is simple and flexible in design, and is able to use multiple harmonics or multiple signals in order to estimate the fundamental frequency of the noise source. In this manner, the algorithm maintains tracking of the fundamental frequency despite significant changes in signal characteristics. The ability of the indirect approach to reject periodic noise with fixed or time-varying frequency and amplitudes is demonstrated in active noise control experiments. The algorithm may also be useful in other control applications where periodic disturbances of unknown frequency must be rejected.

*Key words:* Active noise control; disturbance rejection; adaptive control; periodic signals; phase-locked loop.

---

## 1 Introduction

### 1.1 Background

An active noise control (ANC) system eliminates or reduces noise through destructive interference [1]. In many ANC applications, the noise of interest is narrowband. This paper concentrates on multivariable feedback control of periodic noise which is composed of multiple harmonics with a single fundamental frequency. Such kind of noise may be generated by rotating engines, compressors, fans, and propellers. The frequency of the noise is not known exactly and may be slowly time-varying due to slow changes in rotational speed. The amplitudes of the sinusoidal components of the disturbances may also be slowly varying.

There is a large volume of literature on active noise control with a reference signal (*feedforward control*). Two

general approaches exist for the feedforward control of periodic noise. In the first approach, which dates back to Lueg's original duct noise controller [2], a sensor picks up an "upstream" reference signal that is closely correlated to the primary noise. The reference signal is then used by the controller to produce a proper control signal so that the primary noise is cancelled or attenuated. The scheme has several limitations, such as the possible feedback of the control signal to the reference sensor. However, it can control both broadband and narrowband noise [1].

Another approach exploits the predictable nature of narrowband disturbances to synthesize an internally generated periodic reference signal. The reference information, which is characterized by the fundamental frequency of the noise, is obtained using a non-acoustic sensor such as an accelerometer or tachometer [3]. Two types of internally generated reference signals are commonly used in periodic noise control systems: (1) impulse train with a frequency equal to the fundamental frequency of the periodic noise [3] [4], and (2) sinusoidal waveforms that have the same frequencies as the corresponding harmonic tones to be cancelled. Noise control for multiple sinusoidal components has been proposed using the sum of the sinusoidal components as the ref-

---

<sup>★</sup> This paper was not presented at any IFAC meeting. Corresponding author M. Bodson. Tel.: (801) 581 8590. Fax: (801) 581 5281.

*Email addresses:* [becky.wu@ece.gatech.edu](mailto:becky.wu@ece.gatech.edu) (Biqing Wu), [bodson@ece.utah.edu](mailto:bodson@ece.utah.edu) (Marc Bodson).

reference signal [5], designing control algorithms for each frequency component independently [6] [7], or using a rectangular waveform with the fundamental period equal to the fundamental period of the noise [8].

The feedforward approaches work well in situations where a reference signal is available that is well-correlated with the primary noise, or when the noise frequency can be easily measured using equipment such as a tachometer mounted on the rotating machine that is causing the noise. Nevertheless, in some situations, it is undesirable or too expensive to use reference sensors, and the information that characterizes the noise can only be obtained from the error sensors. Then, a feedback ANC system is needed.

While the rejection of periodic disturbances is a classical problem of feedback control when the frequency of the disturbance is known, few algorithms exist for the case when the frequency is unknown and possibly time-varying. An early reference for feedback control of narrowband noise is the patent of Chaplin and Smith [9], which describes in broad terms the concept of an active noise control system where the frequency of the noise is estimated using a phase-locked loop. The patent does not report analysis, simulation or experimental results, and is not specific about the implementation. However, [10] provides analytical and simulation results for a possible implementation of the concept.

In adaptive control, the terminology “indirect” usually applies to an algorithm where the parameters of the system are estimated, and inserted in a control algorithm using a design procedure that assumes that the estimates are exact. In analogy, Fig. 1 shows the concept of an indirect approach for periodic disturbance rejection which generalizes the approach of [9]. The frequency of the noise is estimated, and the estimate is applied in a scheme for the cancellation of noise of known frequency. In the figure,  $d(t)$  is the effect of noise source at the sensor location,  $u(t)$  is the control input, and  $e(t)$  is the residual error signal picked up by the sensor. The plant is given by  $P(s)$ , which includes the dynamics of the sound propagation from the control actuator to the sensor. The frequency estimate of the noise signal is denoted by  $\omega$ .  $\hat{P}(s)$  is an estimate of the plant transfer function.

Recently, there have been a few attempts at implementing indirect algorithms in active noise control. [11], [12], and [13] report on experimental results obtained with adaptive notch filters for frequency estimation. This paper extends the indirect adaptive algorithm of [14] to a multi-channel noise control system and proposes the use of an alternate frequency estimation method. Experimental results show that, despite high initial uncertainty, the indirect scheme is able to reduce significantly the noise level at the microphone locations. Using the alternate frequency estimation method, the algorithm is also able to maintain consistent performance even when

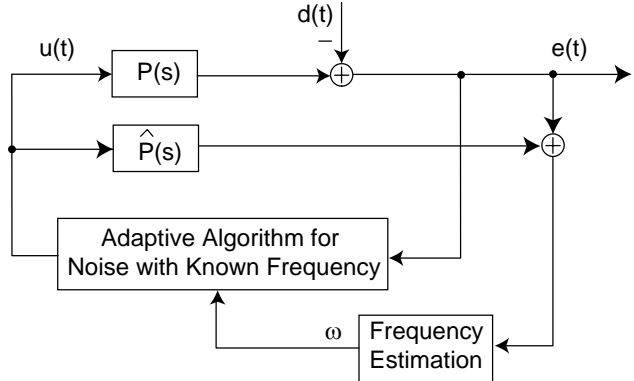


Fig. 1. Indirect approach (SISO Case)

the fundamental component of the measured signal becomes very small or zero.

## 1.2 Problem Statement

Assume that the effect of the noise is additive and that the channels from the actuators to the sensors can be described by a stable, linear time-invariant system with transfer function matrix  $P(s)$ .  $P_{il}(s)$  is the transfer function from control input (speaker)  $\#l$  to residual error (microphone)  $\#i$ . It is assumed that the number of error sensors  $I$  is greater than or equal to the number of control inputs  $L$  in the system, *i.e.*,  $I \geq L$ . This is a typical situation in active noise control systems and many other applications where sensors are cheaper than actuators.

It is assumed that suitable locations for the control sources and the sensors are chosen, so that the system frequency response matrix is of full rank (*i.e.*,  $\mathbf{P}(j\omega)$  has  $L$  linearly independent rows) at the frequencies of the noise signals. For that purpose, it may be assumed that the frequency of the noise is known to lie in a certain range, through which the rank condition can be tested. However, in a system with more sensors than actuators, the condition will typically be satisfied. Let us define the symbols  $u_l(t)$ ,  $e_i(t)$ , and  $d_i(t)$  as the control signals, the sensor signals (or the plant outputs), and the noise signals at the sensor locations, and  $p_{il}(t)$  as the impulse response of the channel transfer function  $P_{il}(s)$ . Defining the vector of error signals  $\mathbf{e}(t)$ , we have

$$\mathbf{e}(t) = \begin{bmatrix} p_{11}(t) & \dots & p_{1L}(t) \\ \vdots & \vdots & \vdots \\ p_{I1}(t) & \dots & p_{IL}(t) \end{bmatrix} * \begin{bmatrix} u_1(t) \\ \vdots \\ u_L(t) \end{bmatrix} + \begin{bmatrix} d_1(t) \\ \vdots \\ d_I(t) \end{bmatrix} \quad (1)$$

where  $*$  denotes linear convolution.

The noise signals  $d_i(t)$  with  $i = 1, \dots, I$  for different sensor locations are assumed to contain multiple harmonics associated with a single fundamental frequency, as is

the case if the source of the disturbances is a rotating machine. The noise signals are represented by

$$d_i(t) = \sum_{m=1}^M \{ \pi_{i,m}^c \cos[m\alpha_d(t)] - \pi_{i,m}^s \sin[m\alpha_d(t)] \} \quad (2)$$

for  $i = 1, 2, \dots, I$ , where  $\alpha_d(t) = \omega_d \cdot t$ , and  $\omega_d$  is the fundamental frequency of the noise. For the purpose of analysis,  $\omega_d$ ,  $\pi_{i,m}^c$ , and  $\pi_{i,m}^s$  are assumed constant. In practice, the parameters may be slowly-varying. The order of the highest harmonic to be cancelled,  $M$ , is assumed to be finite and known.

The objective of the control system is to generate control signals  $u_l(t)$  such that the effects of the disturbance signals at the sensor locations are cancelled through destructive interference. If there are more sensors than actuators (*i.e.*,  $I > L$ , and the system is said to be over-determined), exact cancellation may not be possible even under ideal conditions.

## 2 Multi-Channel Adaptive Cancellation for Sources of Known Frequency

### 2.1 Inverse G algorithm

Algorithms for the control of noises with known frequency form the inner control loop of the indirect scheme presented in this paper. We first consider an adaptive algorithm that we call the inverse G algorithm. It is a pseudo-gradient type of algorithm. In this algorithm, the multiple control sources are given by

$$u_l(t) = \sum_{m=1}^M [\theta_{l,m}^c(t) \cos(m\alpha(t)) - \theta_{l,m}^s(t) \sin(m\alpha(t))] \quad (3)$$

for  $l = 1, 2, \dots, L$ , where we assume that  $\alpha(t) = \alpha_d(t)$ .

To describe the algorithm in a compact form, let us define the control signal vector

$$\mathbf{u}(t) = \begin{bmatrix} u_1(t) & \dots & u_L(t) \end{bmatrix}^T. \quad (4)$$

The corresponding cos and sin amplitude parameter vectors for each harmonic are defined to be

$$\begin{aligned} \boldsymbol{\theta}_m^c(t) &= \begin{bmatrix} \theta_{1,m}^c(t) & \dots & \theta_{L,m}^c(t) \end{bmatrix}^T \\ \boldsymbol{\theta}_m^s(t) &= \begin{bmatrix} \theta_{1,m}^s(t) & \dots & \theta_{L,m}^s(t) \end{bmatrix}^T \end{aligned} \quad (5)$$

for  $m = 1, 2, \dots, M$ .

The parameter vectors  $\boldsymbol{\theta}_m^c(t)$  and  $\boldsymbol{\theta}_m^s(t)$  are then updated according to

$$\begin{bmatrix} \dot{\boldsymbol{\theta}}_m^c(t) \\ \dot{\boldsymbol{\theta}}_m^s(t) \end{bmatrix} = -g (\hat{\mathbf{G}}_m^T \hat{\mathbf{G}}_m)^{-1} \hat{\mathbf{G}}_m^T \begin{bmatrix} \mathbf{e}(t) \cos(m\alpha(t)) \\ -\mathbf{e}(t) \sin(m\alpha(t)) \end{bmatrix} \quad (6)$$

where  $g > 0$  is an arbitrary adaptation gain. The  $2I \times 2L$  matrices  $\hat{\mathbf{G}}_m$  are estimates of the true plant matrices

$$\mathbf{G}_m = \frac{1}{2} \begin{bmatrix} \mathbf{P}_{R,m} & -\mathbf{P}_{I,m} \\ \mathbf{P}_{I,m} & \mathbf{P}_{R,m} \end{bmatrix} \quad (7)$$

and the elements of  $\mathbf{G}_m$  are the plant frequency response values estimated at the frequency of the  $m$ th harmonic of the noise, *i.e.*,

$$\begin{aligned} \mathbf{P}(jm\omega) &= \mathbf{P}_{R,m} + j\mathbf{P}_{I,m} \\ &= \begin{bmatrix} P_{11}(jm\omega) & \dots & P_{1L}(jm\omega) \\ \dots & \dots & \dots \\ P_{I1}(jm\omega) & \dots & P_{IL}(jm\omega) \end{bmatrix} \end{aligned} \quad (8)$$

In practice, the frequency response matrix of the plant is estimated during a preliminary training phase using appropriate signals.

The pseudo-inverse  $(\hat{\mathbf{G}}_m^T \hat{\mathbf{G}}_m)^{-1} \hat{\mathbf{G}}_m^T$  of the non-square matrix  $\hat{\mathbf{G}}_m$  may be implemented using

$$\begin{aligned} (\hat{\mathbf{G}}_m^T \hat{\mathbf{G}}_m)^{-1} \hat{\mathbf{G}}_m^T &= 4 \begin{bmatrix} (\hat{\mathbf{D}}_m + \hat{\mathbf{E}}_m \hat{\mathbf{D}}_m^{-1} \hat{\mathbf{E}}_m)^{-1} \\ -(\hat{\mathbf{D}}_m + \hat{\mathbf{E}}_m \hat{\mathbf{D}}_m^{-1} \hat{\mathbf{E}}_m)^{-1} \hat{\mathbf{E}}_m \hat{\mathbf{D}}_m^{-1} \\ (\hat{\mathbf{D}}_m + \hat{\mathbf{E}}_m \hat{\mathbf{D}}_m^{-1} \hat{\mathbf{E}}_m)^{-1} \hat{\mathbf{E}}_m \hat{\mathbf{D}}_m^{-1} \\ (\hat{\mathbf{D}}_m + \hat{\mathbf{E}}_m \hat{\mathbf{D}}_m^{-1} \hat{\mathbf{E}}_m)^{-1} \end{bmatrix} \hat{\mathbf{G}}_m^T, \end{aligned} \quad (9)$$

with

$$\hat{\mathbf{D}}_m = (\hat{\mathbf{P}}_{R,m}^T \hat{\mathbf{P}}_{R,m} + \hat{\mathbf{P}}_{I,m}^T \hat{\mathbf{P}}_{I,m}) = \hat{\mathbf{D}}_m^T \quad (10)$$

and

$$\hat{\mathbf{E}}_m = \hat{\mathbf{P}}_{R,m}^T \hat{\mathbf{P}}_{I,m} - \hat{\mathbf{P}}_{I,m}^T \hat{\mathbf{P}}_{R,m} = -\hat{\mathbf{E}}_m^T \quad (11)$$

Note that the inverse is well-defined under the assumption made earlier that the plant frequency response matrix has full row rank at the frequency of the  $m$ th harmonic. In real-time implementation, the approximate inverse

$$(\hat{\mathbf{G}}_m^T \hat{\mathbf{G}}_m)^{-1} \hat{\mathbf{G}}_m^T \simeq 4 \begin{bmatrix} \hat{\mathbf{D}}_m & \mathbf{0} \\ \mathbf{0} & \hat{\mathbf{D}}_m \end{bmatrix}^{-1} \hat{\mathbf{G}}_m^T \quad (12)$$

may be used. The inverse is exact if

$$\hat{\mathbf{E}}_m = \mathbf{0}, \text{ or } \hat{\mathbf{P}}_{R,m}^T \hat{\mathbf{P}}_{I,m} = \hat{\mathbf{P}}_{I,m}^T \hat{\mathbf{P}}_{R,m}. \quad (13)$$

This property is satisfied in particular if, for a  $2 \times 2$  system,  $\hat{P}_{11}(jm\omega) = \hat{P}_{22}(jm\omega)$ , and  $\hat{P}_{12}(jm\omega) = \hat{P}_{21}(jm\omega)$ . These conditions may be viewed as ‘‘symmetry’’ conditions, in the sense that the behavior of the system is the same if the order of the inputs and outputs are permuted at the same time. However, experiments show that the approximate inverse is useful even when the symmetry conditions are not exactly satisfied.

## 2.2 Comparison with the Gradient Algorithm

Another commonly used adaptive algorithm for the cancellation of noise with known frequency is the gradient (or FXLMS in [16]) algorithm. To control periodic noises in a multi-channel system, the gradient algorithm designed to minimize the error function  $J(t) = \mathbf{e}^T(t)\mathbf{e}(t)$  consists in

$$\begin{bmatrix} \dot{\boldsymbol{\theta}}_m^c(t) \\ \dot{\boldsymbol{\theta}}_m^s(t) \end{bmatrix} = -g \hat{\mathbf{G}}_m^T \begin{bmatrix} \mathbf{e}(t) \cos(m\alpha(t)) \\ -\mathbf{e}(t) \sin(m\alpha(t)) \end{bmatrix}. \quad (14)$$

A minor adjustment was made to the standard gradient algorithm: the responses of the plant to the in-phase and quadrature components of the control signals were replaced by the steady-state responses using the matrix  $\hat{\mathbf{G}}_m$ . In other words, the plant was modeled by its gains and phase shifts at the individual frequencies.

To compare the convergence properties of both adaptive algorithms, we define the parameter error

$$\boldsymbol{\phi}_m = \begin{bmatrix} \boldsymbol{\theta}_m^c - \boldsymbol{\theta}_m^{c*} \\ \boldsymbol{\theta}_m^s - \boldsymbol{\theta}_m^{s*} \end{bmatrix}, \quad (15)$$

where the nominal values of the parameters are given by

$$\begin{bmatrix} \boldsymbol{\theta}_m^{c*} \\ \boldsymbol{\theta}_m^{s*} \end{bmatrix} = -\frac{1}{2}(\mathbf{G}_m^T \mathbf{G}_m)^{-1} \mathbf{G}_m^T \begin{bmatrix} \boldsymbol{\pi}_m^c \\ \boldsymbol{\pi}_m^s \end{bmatrix}, \quad (16)$$

with

$$\begin{aligned} \boldsymbol{\pi}_m^c &= \begin{bmatrix} \pi_{1,m}^c(t) & \dots & \pi_{I,m}^c(t) \end{bmatrix}^T \\ \boldsymbol{\pi}_m^s &= \begin{bmatrix} \pi_{1,m}^s(t) & \dots & \pi_{I,m}^s(t) \end{bmatrix}^T \end{aligned} \quad (17)$$

for  $m = 1, 2, \dots, M$ . An averaging analysis [15] then shows that, for the inverse G algorithm, the dynamics of the averaged parameter error are given by

$$\dot{\boldsymbol{\phi}}_{av,m} = -g(\hat{\mathbf{G}}_m^T \hat{\mathbf{G}}_m)^{-1} \hat{\mathbf{G}}_m^T \mathbf{G}_m \boldsymbol{\phi}_{av,m}. \quad (18)$$

If there is no modeling error and the frequency estimate is equal to the true value,  $\hat{\mathbf{G}}_m = \mathbf{G}_m$  and we have

$$\dot{\boldsymbol{\phi}}_{av,m} = -g\boldsymbol{\phi}_{av,m}. \quad (19)$$

The result shows that, for small enough  $g$ , the stability of the adaptive system is guaranteed, and that the adaptive parameters in  $\boldsymbol{\theta}_m^c$  and  $\boldsymbol{\theta}_m^s$  converge with identical speeds to their nominal values. The convergence speed is determined by the adaptation gain  $g$  and is independent of the plant response for different noise frequencies. The price to pay for the desirable convergence properties is that the pseudo-inverse of the matrix  $\hat{\mathbf{G}}_m$ , for  $m = 1, 2, \dots, M$ , requires intensive computations when the number of the control signals is large.

For the gradient algorithm, the dynamics of the averaged parameter error are given by

$$\dot{\boldsymbol{\phi}}_{av,m} = -g(\hat{\mathbf{G}}_m^T \mathbf{G}_m) \boldsymbol{\phi}_{av,m}. \quad (20)$$

In the absence of modeling error and frequency error,  $\hat{\mathbf{G}}_m = \mathbf{G}_m$ , and we have

$$\hat{\mathbf{G}}_m^T \mathbf{G}_m = \hat{\mathbf{G}}_m^T \hat{\mathbf{G}}_m = \frac{1}{4} \begin{bmatrix} \hat{\mathbf{D}}_m & \hat{\mathbf{E}}_m^T \\ \hat{\mathbf{E}}_m & \hat{\mathbf{D}}_m \end{bmatrix}. \quad (21)$$

Because the matrix  $\hat{\mathbf{G}}_m^T \hat{\mathbf{G}}_m$  is symmetric and positive definite, the adaptive parameters converge to their nominal values for small enough gain and under ideal conditions. The convergence properties of the adaptive weights  $\boldsymbol{\theta}_m^c$  and  $\boldsymbol{\theta}_m^s$  depend on the multi-channel plant response at the frequency of the  $m$ th harmonic of the noise. For systems in which the matrix  $\hat{\mathbf{G}}_m^T \hat{\mathbf{G}}_m$  is ill-conditioned (*i.e.*, the eigenvalues of the matrix have a wide range of values), the convergence of the algorithm is slowed down by the modes associated with small eigenvalues, since the adaptation gain must be kept small enough that the modes associated with large eigenvalues remain stable.

The distribution in eigenvalues for a given frequency is related to the spatial positioning of the control sources and the error sensors. If the noise frequency varies, there will be a variation of the eigenvalues with time, which may be significant if the magnitude responses of the plant transfer functions have strong peaks and valleys as is often the case in active noise control in an enclosure. Convergence properties of the gradient algorithm will be further degraded. However, the advantage of the algorithm is that the matrix inverse is not required.

## 2.3 Normalized Gradient Algorithm

The inverse G algorithm with approximate inverse was defined by (6) and (12). The algorithm may be viewed

as a normalized form of the gradient algorithm (14). The computational requirement of the matrix inverse can be further reduced by approximating  $\hat{\mathbf{D}}_m$  by its diagonal, whose elements are

$$\hat{D}_{l,m} \simeq \sum_{i=1}^I |P_{il,m}(jm\omega)|^2 \quad (22)$$

The approximation normalizes the gradient algorithm, resulting in more consistent convergence performance along the spectral dimension, while the spatial variation is not addressed. The normalized algorithm is a trade-off between the inverse  $G$  algorithm and the gradient algorithm.

### 3 Frequency Estimation Method

#### 3.1 Frequency Estimation Signal

The effect of the control signals is subtracted from the error signal before the resulting signal  $y_1(t)$  is used to estimate the frequency, as illustrated in Fig. 2 for a 2-channel noise control system. In the figure,  $\hat{P}_{11}(s)$  and  $\hat{P}_{12}(s)$  are the estimates of the plant transfer functions  $P_{11}(s)$  and  $P_{12}(s)$ , respectively, and  $\omega$  is the estimated fundamental frequency of the noise. It was found that, unlike internal model control (IMC) [17] [18], the estimates of the plant transfer functions did not have to be precise in order for this approach to work well.

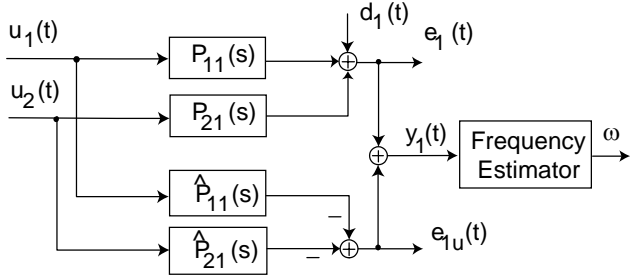


Fig. 2. Construction of frequency estimation signal

#### 3.2 Adaptive Notch Filter

An adaptive notch filter [19] transposed to continuous-time form was used to estimate the frequency of a sinusoidal signal in [14]. The continuous-time notch filter is given by:

$$N(s) = k \frac{s^2 + \omega^2}{s^2 + 2\zeta\omega s + \omega^2}, \quad (23)$$

where  $k$  is the filter gain and  $\zeta$  is the damping factor that determines the bandwidth of the filter's notch. The sinusoidal signal is filtered through the notch filter, while

the notch frequency  $\omega$  is adapted to minimize the output of the notch filter. The adaptive notch filter is described by differential equations with three states  $\omega$ ,  $x_1$ , and  $x_2$ :

$$\begin{aligned} \dot{x}_1 &= x_2 \\ \dot{x}_2 &= -2\zeta\omega x_2 - \omega^2 x_1 + ky_1 \\ \dot{\omega} &= -g_1(ky_1 - 2\zeta\omega x_2)x_1 \end{aligned} \quad (24)$$

where  $g_1$  is the adaptation gain. The algorithm's behavior was explained through an averaging analysis in [14], assuming a small value of  $g_1$ . It was found that the frequency estimate  $\omega$  converged without bias to the true value when  $y_1(t)$ , which is one of the sensor signals processed in the way as shown in Section 3.1, contained a single sinusoid. When the input  $y_1(t)$  contained multiple sinusoids, the frequency estimate  $\omega$  converged to the most significant frequency that was in the vicinity of the initial value of  $\omega$ . The estimation bias depended on the damping factor  $\zeta$ , and the bias tended to zero as  $\zeta \rightarrow 0$ .

#### 3.3 Phase-Locked Loop

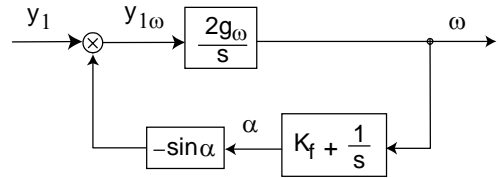


Fig. 3. Frequency estimation based on phase-locked loop

The phase-locked loop technique [20] is simple and effective for estimation and tracking of time-varying frequency [21]. Fig. 3 shows a phase-locked loop described by

$$\begin{aligned} \alpha(t) &= K_f \omega(t) + \int_0^t \omega(\tau) d\tau, \\ \dot{\omega}(t) &= 2g_\omega y_1(t) (-\sin(\alpha(t))). \end{aligned} \quad (25)$$

The design parameters  $K_f$  and  $g_\omega$  are both positive. Note that the phase  $\alpha$  is not purely integrated from the frequency estimate  $\omega$ , as is usually done in phase-locked loops [20]. The additional proportional term with gain  $K_f$  provides the phase lead that is typically incorporated through a lead filter.

If the high frequency terms of the variable  $y_{1\omega}$  are discarded, and the frequency estimate  $\omega$  is close enough to the fundamental frequency  $\omega_d$ , the dynamics of the linear approximate of the loop are those of a second-order system with poles determined by the roots of

$$s^2 + g_\omega m_{1d} K_f s + g_\omega m_{1d} = 0, \quad (26)$$

where  $m_{1d}$  is the magnitude of the fundamental component of the signal. Stability is guaranteed as the values of  $K_f$  and  $g_\omega m_{1d}$  are both positive.

### 3.4 Modified Phase-Locked Loop

In the above estimator, only the information obtained from the fundamental component of one signal is used. However, in some situations, the fundamental component of the signal may become small for some frequencies. In active noise control in a confined environment, the transfer function of a primary plant (from a noise source to a microphone) often exhibits zeros of transmission (exact or approximate) at certain frequencies. Any component of the noise signal at the microphone may therefore disappear temporarily as the fundamental frequency of the noise varies. [12] proposes a frequency estimation algorithm using a cascade adaptive notch filter to solve the problem. The algorithm rejects erroneous estimation results caused by the disappearance of some noise components using decision rules. In contrast, the algorithm discussed here uses the integral factors between the frequencies of the harmonics so that the multiple components all contribute to a single frequency estimate. The information provided by multiple components is *combined*, and no decision rules are required. As transmission zeros from a noise source to different microphones usually occur at different frequencies, performance improvement may also be achieved by combining different microphone signals in the frequency estimation.

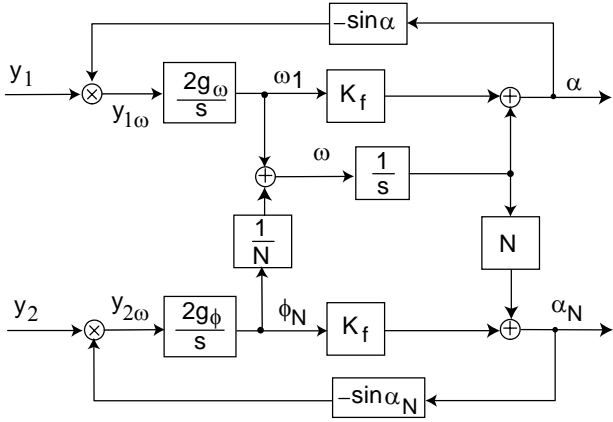


Fig. 4. Frequency estimation based on a modified PLL

Fig. 4 shows a modified phase-locked loop for such purpose [22]. The algorithm uses the fundamental component of  $y_1$  and the  $N$ th harmonic of  $y_2$  in the frequency estimation. For  $N = 1$ , the figure shows an algorithm that uses the fundamental components of two microphone signals  $y_1$  and  $y_2$ . For  $y_1 = y_2$ ,  $N \neq 1$ , the figure shows an algorithm that uses the fundamental and the  $N$ th component of one microphone signal  $y_1$ . Extension to arbitrary combinations of signals and/or harmonics may easily be derived. The equations for Fig. 4 are

$$y_{1\omega} = y_1(-\sin(\alpha)), \quad y_{2\omega} = y_2(-\sin(\alpha_N))$$

$$\begin{aligned} \dot{\omega}_1 &= 2g_\omega y_{1\omega}, \quad \dot{\phi}_N = 2g_\phi y_{2\omega}, \quad \omega = \omega_1 + \frac{1}{N}\phi_N \\ \alpha &= K_f \omega_1 + \int_0^t \omega dt, \quad \alpha_N = K_f \phi_N + N \int_0^t \omega dt, \end{aligned} \quad (27)$$

where the design parameters  $K_f$ ,  $g_\omega$ , and  $g_\phi$  are all positive.

Analysis [22] shows that the dynamics of the linear approximation of the loop are those of a third-order system, with poles determined by the roots of

$$(s + g_\omega m_{1d} K_f)(s^2 + g_\phi m_{Nd} K_f s + g_\phi m_{Nd}) + g_\omega m_{1d}(s + g_\phi m_{Nd} K_f) = 0, \quad (28)$$

where  $m_{Nd}$  is the magnitude of the  $N$ th component of  $y_1$ . Application of the Routh-Hurwitz test shows that the closed-loop poles are stable for all positive values of  $K_f$ ,  $g_\omega$ , and  $g_\phi$ . Some prior knowledge about the value range of  $m_{1d}$  and  $m_{Nd}$  is useful to guarantee the desired performance of the system. If  $g_\omega$  and  $g_\phi$  are chosen such that  $g_\omega m_{1d} = g_\phi m_{Nd}$ , the characteristic equation is given by

$$(s + g_\omega m_{1d} K_f)(s^2 + g_\omega m_{1d} K_f s + 2g_\omega m_{1d}) = 0, \quad (29)$$

which helps to place the poles appropriately.

If one of the two components vanishes, the dynamics of the estimator reduce to those of the phase-locked loop method of Section 3.3 that is based solely on the non-zero component. The combination of the multiple components of different microphone signals in the frequency estimation makes the estimator more flexible, as it is not necessary to know *a priori* which component exists or is the most suitable to base the estimation on. The modified algorithm is especially useful when the magnitudes of the noise signals change with time.

## 4 Experimental Testbed and Plant Modeling

The schemes for rejection of periodic signals were implemented on an experimental active noise control system developed at the University of Utah. The algorithm was coded in the assembly language of Motorola's DSP96002 32-bit floating-point digital signal processor hosted in a PC. The sampling rate was set at 8 kHz. A single bookshelf speaker with a 4-inch low-frequency driver generated the periodic signal constituting the noise source. The signals were collected by two microphones separated by about 2.7 ft (0.82m). These signals were passed through anti-aliasing filters and sampled by self-calibrating 16-bit analog-to-digital converters before being sent to the DSP system. The controller output signals were sent to two noise cancelling speakers positioned symmetrically with respect to the microphones.

The whole system was set at about 2 ft (0.61m) in height in a small room.

The algorithms require knowledge of the frequency response matrix  $\mathbf{P}(j\omega)$  of the plant for the frequency estimation as well as for the adaptive cancellation. Assuming that the characteristics of  $\mathbf{P}(j\omega)$  are time-invariant but unknown, measurements can be used to estimate  $\mathbf{P}(j\omega)$  during an initial training stage. At the end of the training interval, the estimated model  $\hat{\mathbf{P}}(j\omega)$  is fixed and used for disturbance rejection operation. The frequency response at a given frequency  $\omega_0$  was determined by the Empirical Transfer Function Estimate (ETF, [23]). Let the first input (produced by control speaker #1) be a pure sinusoid  $\cos(\omega_0 n)$  and the second input (produced by control speaker #2) be zero.  $\hat{\mathbf{P}}_1(j\omega_0)$ , which is the first column of  $\hat{\mathbf{P}}(j\omega_0)$ , was obtained through

$$\begin{aligned} \text{Re}(\hat{\mathbf{P}}_1(j\omega_0)) &= \frac{2}{N} \sum_{n=1}^N \mathbf{E}(n) \cos(\omega_0 n) \\ \text{Im}(\hat{\mathbf{P}}_1(j\omega_0)) &= -\frac{2}{N} \sum_{n=1}^N \mathbf{E}(n) \sin(\omega_0 n) \end{aligned} \quad (30)$$

where  $\mathbf{E}(n)$  is the vector of plant outputs, and  $N = k\pi/\omega_0$  with  $k = 1, 2, 3, \dots$ .

The second column of  $\hat{\mathbf{P}}(j\omega_0)$  may be obtained similarly. In the implementation of the algorithm, it was assumed that  $P_{11}(j\omega) = P_{22}(j\omega)$ , and  $P_{12}(j\omega) = P_{21}(j\omega)$ , even though the real plant did not satisfy the symmetry requirement. This assumption need not be made in general, but the complexity of the code is reduced if the assumption is used. In the experiment, the real and imaginary parts of the frequency response were obtained at 64 different frequencies, spaced between 90 Hz and 375 Hz, and the results were saved in a look-up table. In real-time operation, the frequency response at the estimated frequency was obtained by linearly interpolating the look-up table, and the matrices  $\hat{\mathbf{G}}_m$  were adjusted continuously as functions of the frequency estimate.

The phase responses of the plant mostly consisted of the linear phase associated with the delay due to sound propagation from the speakers to the microphones. The magnitude responses showed a significant number of peaks and valleys, which were attributed to acoustic resonances in the small room that was used for experimentation. At valley frequencies, the actuator of a single-channel control system needs a control output of high volume in order to cancel the noise. The actuator may become saturated and cause a stability problem. A solution to this problem is to use a multi-channel control system such as developed in this paper.

## 5 Experimental Results

### 5.1 Comparison of Frequency Estimation Algorithms

The inverse  $G$  algorithm was implemented as the inner loop of the indirect scheme, using the approximate inverse of the matrix  $\hat{\mathbf{G}}_m$  given by equation (12). The noise signals contained a fundamental and a 2nd harmonic. First, the fundamental frequency was fixed at 130 Hz. The experimental results showed that the algorithm, combined with any one of the three frequency estimation methods, reduced both noise signals considerably within one second after the control effort was engaged. The periodic components of the two noise signals were completely eliminated. In a different experiment, the fundamental frequency of the noise was increased linearly from 130 Hz to 150 Hz in 10 seconds. Due to the acoustic properties of the room, the amplitudes of the noise signals at the two microphone locations changed as a function of frequency. The design parameters of the control algorithm were chosen to maximize the tracking speed, while keeping the adaptive system stable. Overall, the contribution of the fundamental component was reduced by approximately 25 dB, and the 2nd harmonic by 18 dB using the adaptive notch filter, and approximately 40 dB and 20 dB using the phase-locked loop and the modified phase-locked loop.

### 5.2 Comparison of Inner Control Loop Algorithms

For comparison, the gradient algorithm and the normalized gradient algorithm were also implemented as the inner control loop algorithm of the indirect scheme. The adaptive notch filter was used to estimate the frequency in this comparison. Table 1 shows the steady-state noise reductions. When the noise frequency was constant, the inverse  $G$  algorithm had better noise reductions than the gradient algorithm, and the convergence speed was faster (the inverse  $G$  algorithm converged in less than 1 second, while the gradient algorithm converged in 2 seconds). When the noise frequency was increasing linearly, the parameters of the gradient and the normalized gradient algorithms were also chosen to maximize the tracking speed, while keeping the adaptive system stable. Again, the inverse  $G$  algorithm had better noise reduction performance than the gradient algorithm. The performance of the normalized gradient algorithm was intermediate, and was more consistent for varying frequencies, although not as good as the inverse  $G$  algorithm.

### 5.3 Experimental Results with Approximate Transmission Zero

To demonstrate the benefits of the modified phase-locked loop in some special situations, experiments were conducted where the fundamental component of the signal became very small. The noise produced by the noise

Freq.	Signal	Comp.	Inv. G	Grad.	Norm.
Constant	#1	fund.	44 dB	19 dB	33 dB
		2nd	38 dB	24 dB	28 dB
	#2	fund.	40 dB	19 dB	32 dB
		2nd	30 dB	18 dB	25 dB
Linear Increase	#1	fund.	25 dB	15 dB	20 dB
		2nd	18 dB	5 dB	10 dB
	#2	fund.	28 dB	18 dB	24 dB
		2nd	18 dB	3 dB	10 dB

Table 1  
Noise reductions using different inner control loop algorithms

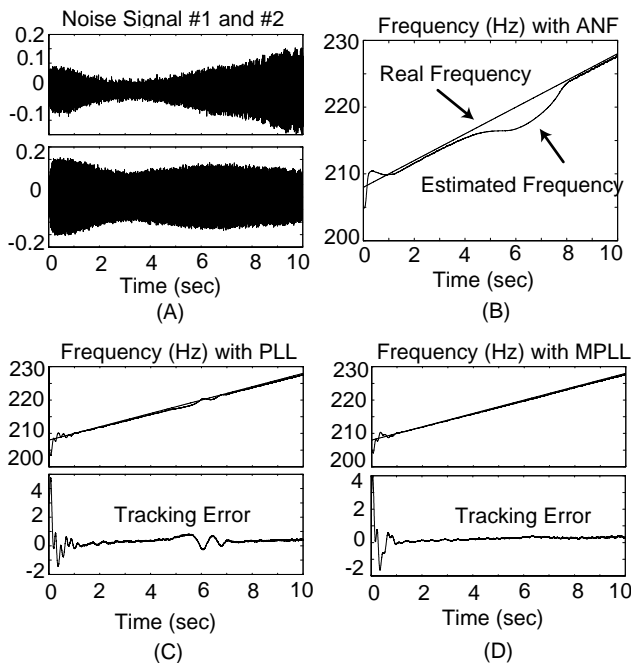


Fig. 5. Noise signals with linear frequency and frequency tracking — approximate zero of transmission encountered at 3 seconds

speaker contained only a fundamental component with a frequency linearly increasing from 208 Hz to 228 Hz in 10 seconds. Fig. 5 (A) shows the noise signals observed at microphone locations #1 and #2 when the control effort was not applied. The amplitudes of the noise signals at the two microphone locations changed slowly, even though the amplitude of the noise source was fixed. The noise signal at microphone #1 became very small temporarily at about 3 seconds, while the noise at microphone #2 location was still significant. An approximate zero of transmission from the noise source to microphone #1 occurs at around 214 Hz, while the response to microphone #2 does not have a zero at the same frequency.

Fig. 5 (B), (C), and (D) show the frequency estimates obtained using the adaptive notch filter, the phase-locked loop, and the modified phase-locked loop, respectively.

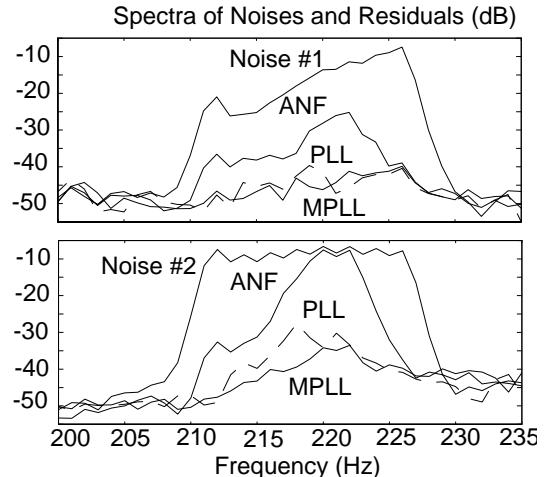


Fig. 6. Spectra of noise signals and their residuals with different frequency estimation methods

In the modified phase-locked loop, noise signal #2 was used together with noise signal #1 in the fundamental frequency estimation. The performance of the frequency tracking is excellent, despite the changing amplitude of the noise signal #1. The experiments demonstrate the ability of the modified phase-locked loop to use multiple signals in order to better estimate the fundamental frequency.

Fig. 6 shows the spectra of the noise signals and the corresponding residual error signals obtained from microphones #1 and #2. The signals after 1.5 seconds were used in the spectral analysis in order to compare the performance of the control system with different frequency estimation methods. The noise signals shown in the spectra have, therefore, significant spectral band from 211 Hz to 228 Hz. The figure shows that the indirect scheme with the adaptive notch filter had the least noise reduction. The indirect schemes with the phase-locked loop and the modified phase-locked loop were both effective overall. The scheme with the modified phase-locked loop had somewhat better performance. Its transient response in the first second of the experiment was also superior to that of the phase-locked loop. Experiments were also conducted where the design parameters were varied within some range while the stability of the control system was maintained. It was found that the above experimental results were typical for the indirect scheme with each of the three frequency estimation methods.

#### 5.4 Experimental Results with Vanishing Fundamental

An even more extreme situation was considered, where the fundamental was made to vanish for some period of time. In the experiments, the control algorithm was engaged after 1 second. The noise contained the fundamental and 2nd harmonic component, until after 5 seconds when the fundamental component became zero. The fundamental frequency of the noise was fixed at 130 Hz.

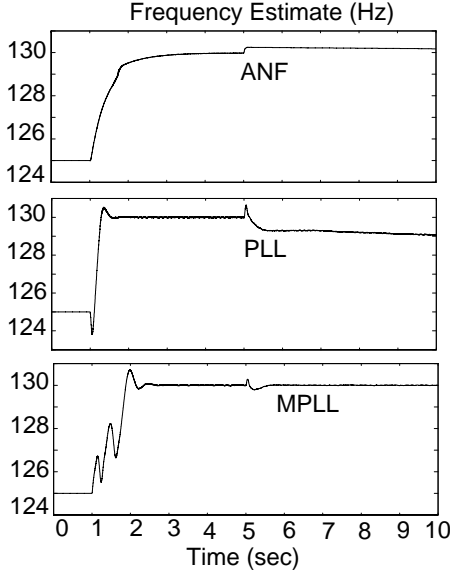


Fig. 7. Frequency estimate when the fundamental component of the noise vanishes after 5 seconds

Since the adaptive notch filter and the phase-locked loop both estimate the frequency using information obtained from the fundamental component, they may be expected to have inferior performance compared to the modified phase-locked loop, which exploits information obtained from the fundamental and the 2nd harmonic component of the noise. The experiments of this section confirm this statement.

Fig. 7 shows the frequency estimates using the adaptive notch filter, the phase-locked loop, and the modified phase-locked loop. The frequency estimate using the adaptive notch filter was biased and attracted to the frequency of the 2nd harmonic after 5 seconds. The frequency estimate using the phase-locked loop also drifted away from the fundamental frequency of the noise after 5 seconds. In the modified phase-locked loop, the 2nd harmonic of microphone signal #1 was used together with the fundamental component for frequency estimation. The second microphone signal was not used for frequency estimation. The estimate of the modified phase-locked loop keeps lock on the fundamental frequency of the noise even when the fundamental component disappeared.

Table 2 shows the steady-state power levels of the residual error signals. In the table, stage #1 denotes the experiment stage from second 1 to 5. Stage #2 means the time period from second 5 to 10. The approximate noise levels before the control effort was engaged is shown in the 3rd column of the table. The background noise of the signals was about  $-50$  dB, so a power level of  $-55$  dB of some component means that the component was completely eliminated or did not exist.

As shown in the table, the indirect scheme with the

Stage	Signal	Component (original dB)	ANF (dB)	PLL (dB)	MPLL (dB)
#1	#1	fund. (1 dB)	-32	-55	-55
		2nd (-1 dB)	-37	-55	-50
	#2	fund. (-1 dB)	-34	-55	-55
		2nd (-10 dB)	-40	-50	-55
#2	#1	fund. (-55 dB)	-55	-55	-55
		2nd (-1 dB)	-20	-13	-50
	#2	fund. (-55 dB)	-55	-55	-55
		2nd (-10 dB)	-23	-16	-55

Table 2  
Noise levels using different frequency estimation methods

modified phase-locked loop was able to eliminate completely the noise at the two microphone locations, for both stages. The schemes with the adaptive notch filter and the phase-locked loop were not as effective in the noise reduction in stage #2, although they were able to eliminate the noise in stage #1. The non-ideal performance of the scheme with the adaptive notch filter at stage #1 shown in the table was due to the slow convergence caused by the small value of  $g_1$ . Increasing the value of  $g_1$  increased the convergence rate and thereby the noise reduction at stage #1. However, the frequency estimation bias at stage #2 was larger and eventually led to instability.

## 6 Conclusions

A feedback active noise control algorithm was presented for multi-channel systems and periodic noise of unknown frequency. The fundamental approach of the proposed indirect control scheme consisted in estimating the frequency of the noise and using the estimate in an adaptive noise control scheme designed for a known frequency. For the inner control loop, an adaptive algorithm called inverse  $G$  algorithm was proposed and its properties were compared through analysis with those of a gradient algorithm. It was found that the convergence speed of the gradient algorithm was limited by the conditioning number of the plant frequency response matrix, while the inverse  $G$  algorithm avoided the problem by introducing the pseudo-inverse of the matrix in the adaptive algorithm. As a result, the inverse  $G$  algorithm converged faster and had better disturbance attenuation performance, especially when the frequency of the disturbances was time-varying. However, the gradient algorithm had the advantage of lower computational complexity, especially when the number of the control actuators was large. A normalized gradient algorithm provided an intermediate solution, both in terms of computational complexity and disturbance reduction performance.

For the frequency estimation, a modified phase-locked

loop was used that was capable of estimating the frequency of the noise signal even when some component of the signal vanished or became small for some periods of time. An attractive feature of the algorithm was that it could combine information obtained from multiple harmonics and/or sensors. Overall, the experimental results showed that the indirect approach was efficient in the multi-channel rejection of periodic noise with fixed or time-varying frequency.

## Acknowledgements

This material is based upon work supported by the National Science Foundation under Grant No. ECS0115070.

## References

- [1] S. M. Kuo and D. R. Morgan, *Active Noise Control Systems: Algorithms and DSP Implementations*, Wiley, New York, 1996.
- [2] P. A. Nelson and S. J. Elliott, *Active Control of Sound*, Academic Press, New York, 1992.
- [3] B. Chaplin and R. Smith, "Waveform Synthesis—the Essex Solution to Repetitive Noise and Vibration," in *Proc. Inter-noise*, 1983, pp. 399-402.
- [4] S. Elliott and P. Darlington, "Adaptive Cancellation of Periodic, Synchronously Sampled Interference," *IEEE Trans. Acoust., Speech, Signal Processing*, ASSP-33, 1985, pp. 715-717.
- [5] J. Glover, Jr., "Adaptive Noise Canceling Applied to Sinusoidal Interferences," *IEEE Trans. Acoust., Speech, Signal Processing*, ASSP-25, 1977, pp. 484-491.
- [6] S.M. Lee, H.J. Lee, C.H. Yoo, D.H. Youn and I.W. Cha, "An active noise control algorithm for controlling multiple sinusoids", *Journal of the Acoustical Society of America*, 104(1), 1998, pp. 248-254.
- [7] X Qiu and C. Hansen, "An algorithm for active control of transformer noise with on-line cancellation path modelling based on perturbation method," *Journal of Sound and Vibration* 240(4), 2001, pp. 647-665.
- [8] P. Hill, "Active Acoustic Attenuation System for Reducing Tonal Noise in Rotating Equipment," U.S. Patent, 5,010,576, 1991.
- [9] G. Chaplin and R. Smith, "Method of and Apparatus for Cancelling Vibrations from a Source of Repetitive Vibrations," U.S. Patent 4,566,118, 1986.
- [10] M. Bodson, "A Discussion of Chaplin & Smith's Patent for the Cancellation of Repetitive Vibrations," *IEEE Trans. on Automatic Control*, vol. 44, no. 11, 1999, pp. 2221-2225.
- [11] L.J. Brown, Q. Zhang, & X. Zhang, "Identification of Periodic Signals with Uncertain Frequency," *Proc. of the American Control Conference*, Anchorage, AK, 2002, pp. 1526-1531.
- [12] S. Kim & Y. Park, "On-Line Fundamental Frequency Tracking Method for Harmonic Signal and Application to ANC," *Journal of Sound and Vibration*, vol. 241, no. 4, 2001, pp. 681-691.
- [13] B. Wu and M. Bodson, "Multi-Channel Active Noise Control for Periodic Disturbances", *Proc. Conference on Decision and Control*, Phoenix, AZ, 1999, pp. 4971-4975.
- [14] M. Bodson and S. Douglas, "Adaptive Algorithms for the Rejection of Sinusoidal Disturbances with Unknown Frequency," *Automatica*, vol. 33, no. 12, 1997, pp. 2213-2221.
- [15] S. Sastry and M. Bodson, *Adaptive Control: Stability, Convergence, and Robustness*. Prentice-Hall, Englewood Cliffs, NJ, 1989.
- [16] S. J. Elliott, C. C. Boucher, and P. A. Nelson, "The Behavior of a Multiple Channel Active Control System," *IEEE Trans. Signal Processing*, vol. 40, 1992, pp. 1041-1052.
- [17] S. J. Elliott and T. J. Sutton, "Performance of Feedforward and Feedback Systems for Active Control," *IEEE Trans. Speech and Audio Processing*, vol. 4, 1996, pp. 214-223.
- [18] W. Tseng, B. Rafaely, and S. J. Elliott, "Combined Feedback-feedforward Active Control of Sound in a Room", *J. Acoust. Soc. Am.*, vol. 104, no. 6, 1998, pp. 3417-3425.
- [19] P. A. Regalia, "An Improved Lattice-Based Adaptive IIR Notch Filter," *IEEE Trans. Signal Processing*, vol. 39, no. 9, 1991, pp. 2124-2128.
- [20] J. Stensby, *Phase-Locked Loops: Theory and Applications*, Boca Raton, Fla., CRC Press, 1997.
- [21] B. Wu and M. Bodson, "A Magnitude/Phase Locked Loop Approach to Parameter Estimation of Periodic Signals", *Proc. of the American Control Conference*, Arlington, VA, 2001, pp. 3594-3599.
- [22] B. Wu and M. Bodson, "Frequency Estimation Using Multiple Sources and Multiple Harmonic Components", *Proc. of the American Control Conference*, Anchorage, AK, 2002, pp. 21-22.
- [23] L. Ljung and T. Glad, *Modeling of Dynamic Systems*, Prentice Hall, Englewood Cliffs, New Jersey, 1993.